A Novel Electric Insulation String Structure With High-Voltage Insulation and Wireless Power Transfer Capabilities

Cheng Zhang, *Member, IEEE*, Deyan Lin, *Member, IEEE*, Niang Tang, and S. Y. Ron Hui, *Fellow, IEEE*

***Abstract*—High-voltage insulation (HVI) strings are commonly used to hold high-voltage electric cables and electrically isolate them from the grounded transmission tower. In this paper, a novel concept of an electric insulation string with HVI and wireless power transfer (WPT) capabilities is presented. Based on the concept of the domino-resonator WPT system, this new structure consists of coil resonators embedded inside totally sealed insulation discs, which are then connected in series to form the new insulation string structure with the simultaneous HVI and WPT functions. This structure allows energy harvested from the ac magnetic field around the high-voltage cable to be transmitted wirelessly to power an online monitoring system in high-voltage transmission tower continuously, thereby reducing the storage requirements of the battery. The design and analysis of this new WPT structure based on the dimensions of commercially available HVI rod are included. Practical measurements obtained from a hardware prototype of about 25 W have been obtained to confirm the WPT capability of the proposal. An energy efficiency of more than 60% has been achieved for a transmission distance of 1.1 m over a wide range of load.**

***Index Terms*—High-voltage insulation (HVI) string, magnetic resonance, wireless power transfer (WPT).**

I. Introduction

THE dawn of the smart grid and Internet of Things eras has prompted active research in recent years to set up online monitoring systems for power transmission systems. Such monitoring systems are particularly important and critical to some regions such as China, which suffered several large-scale blackouts in recent years due to heavy snow storms in central and northern China [1] and typhoons in southern China [2]. The 2008 power blackout in China [1] has resulted in a total financial loss exceeding RMB 100 billion (approx. US$ 15 billion) [7]. The seriousness of the power blackout problems in China is reflected in our literature review using IEEE Xplore that the majority of recent publications (since 2008) related to online monitoring research of power transmission towers actually came from China. Online monitoring systems for power transmission towers and cables cover a range of monitoring services such as electric parameters (e.g., voltage, current, phase angle, and power) [3], mechanical parameters (e.g., tower structure [4], cable galloping, ice/snow thickness [5]–[7], and wind-induced mechanical vibration of transmission tower [8]), thermal parameters (e.g., cable temperature) [4] and weather information (e.g., wind speed, temperature and lightning, and pollution level) [7], [9], [10] as well as antitheft monitoring [11]. With the increasing requirements for online monitoring, there is a need for providing reliable power supply to power the monitoring instruments. In the past, solar power was the dominant power source. However, with several years of practical installations, power companies such as Guangdong Power have concluded that solar power is not the optimal solution for several reasons. First, there are prolonged periods of rainy and cloudy days that make solar power alone unsuitable from a reliability point of view. Second, solar energy harvesting is only possible during day time when the weather is good, meaning that the size of the battery storage has to be large. In view of the increasing demand for powering online monitoring systems for power transmission towers and transmission lines, this project focuses on the following:

1) "Reliable and continuous" energy harvesting from the HV transmission lines;
2) "High-efficiency wireless power transfer (WPT)" between any two points that require large creepage distance for HV insulation reasons.

A literature review conducted for this project indicates that energy harvesting can be achieved via photovoltaic (PV), wind, electric field, and magnetic field for power transmission systems. So far, very limited work has been reported on techniques for transferring power over the creepage distance (typically from tens of centimeters to a few meters) in HV power transmis-

Manuscript received January 4, 2017; revised March 29, 2017; accepted May 4, 2017. Date of publication May 18, 2017; date of current version October 6, 2017. This work was supported by the Hong Kong Research Grant Council under Project 17255916. Recommended for publication by Associate Editor C. Fernandez *(Corresponding author: S. Y. Ron Hui.)*

C. Zhang was with the Department of Electrical and Electronic Engineering, The University of Hong Kong, Hong Kong. He is now with the Research Laboratory of Electronics, Massachusetts Institute of Technology, Cambridge, MA 02139 USA (e-mail: guszhang@mit.edu).

D. Lin was with the Department of Electrical and Electronic Engineering, The University of Hong Kong, Hong Kong. He is now with the School of Automation, Wuhan University of Technology, Wuhan 430070, China (e-mail: deyanlin@whut.edu.cn).

N. Tang is with the Electric Power Research Institute, Guangdong Power Grid Corporation Ltd., Guangzhou 510080, China (e-mail: tangniang84@163.com).

S. Y. R. Hui is with the Department of Electrical and Electronic Engineering, Imperial College London, London SW7 2AZ, U.K., and also with the Department of Electrical and Electronic Engineering, The University of Hong Kong, Hong Kong (e-mail: ronhui@eee.hku.hk).

This paper has supplementary downloadable material available at http://ieeexplore.ieee.org. This material is 58.3 MB in size.

Color versions of one or more of the figures in this paper are available online at http://ieeexplore.ieee.org.

Digital Object Identifier 10.1109/TPEL.2017.2706221

sion towers and cables. The only exception seems to be the microwave technique mentioned in [12], in which microwave repeaters are used to transmit power harvested from the power cables from one point to another. Therefore, technology for safe and efficient power transfer over long creepage distance in HV power transmission systems is a largely unchartered research area.

Midrange WPT techniques have been proposed in the last decade. The magnetic resonance principle used recently in [13] was not new because Tesla used magnetic resonance in his early WPT experiments [25]. The limitation in [13] is that it adopts the maximum power transfer principle. For any circuit that operates with the maximum power transfer theorem via impedance matching with the source impedance, there is an inherent limitation that the energy efficiency of the system cannot be higher than 50%. For a transmission distance of about 2 m and using coils with large diameters, the system energy efficiency in [13] is only 15%. This serious limitation has been explained in a review paper [14]. A pair of dipole coils has been adopted for WPT of 209 W over 5 m at an energy efficiency of 8% [26]. On the other hand, the wireless domino-resonator systems have been practically proven [15]–[18] to be a highly efficient way to transfer wireless power over a few meters. Unlike the proposal in [13], the wireless domino-resonator systems adopt the maximum energy efficiency principle and can achieve an overall system energy efficiency higher than 50%.

In this paper, the domino-resonator concept is incorporated into a new structure of electric insulation rod or string, which offers the dual capabilities of high-voltage insulation (HVI) and WPT. Coil resonators are resonant tanks formed by connecting a coil (inductor) and a resonant capacitor. They can be embedded in HV insulation discs to form a new insulation string with HVI and WPT capabilities. For the first time, coil resonators are designed to fit into the interior space of commercially available high-voltage insulator rod with standard dimensions for HVI. A hardware prototype with rated power of 25 W has been constructed for practical evaluation so that the WPT capability of the insulation rod can be studied in a realistic manner. Experimental results show that an energy efficiency above 60% can be achieved for WPT for a transmission distance of 1.1 m. This paper is an extended version of a short conference paper previously presented in [19]. The analysis points to a new design approach to operating the system within a high energy efficiency region in order to avoid problem arising from parametric tolerance. A full section on experimental verification is included.

II. Requirements of Online Monitoring System for Power Transmission Systems

Previous online monitoring was powered by PV systems that have several limitations. First, energy harvesting is limited to a few hours each day and is ineffective in prolonged period of cloudy or rainy weather. Second, the short duration of solar energy harvesting means that large battery storage is required. The failure to monitor faults in the prolonged snow storm period in 2008 exposed these fatal problems. Take a simple example.

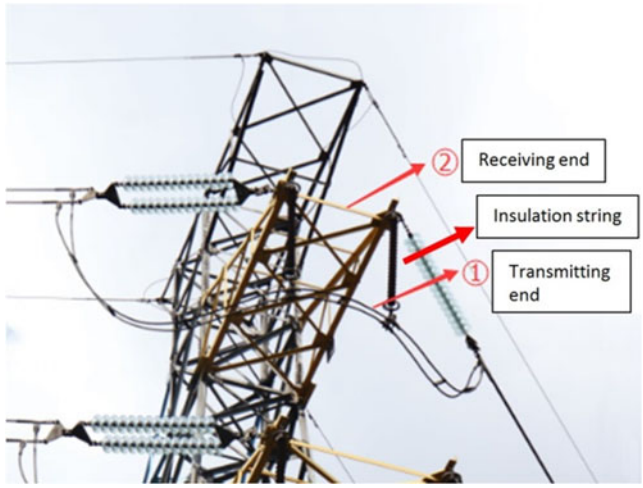

Fig. 1. Energy harvesting point at the shielded cable: ① and Energy receiving point and ② at the tower structure. [Note: There is a large creepage distance between ① and ②].

TABLE I
IEC 60137 Standard on Creepage Distance for Voltage > 1000 V

Condition	Creepage
Normal	16 mm/kV
Medium pollution	20 mm/kV
Heavy pollution	25 mm/kV
Very heavy Pollution	31 mm/kV

If a PV system can harvest an average of 6 h of solar energy each day under normal situation, the battery needs to provide 450 V Ah to power an online monitoring equipment of 25 W for the remaining 18 h. Under the same normal situation, the proposed system harvests energy continuously from the magnetic field around the transmission cable and therefore theoretically does not need any battery storage. In practice, a small battery is needed so that the online monitoring system can wirelessly transmit fault signals and locations to the control center if abnormal situation occurs.

The new concept of this proposal can be illustrated with the aid of a practical transmission tower example shown in Fig. 1. The magnetic field generated by the transmission cable (marked as ① in Fig. 1) can be "continuously" harvested with a transformer and a power converter. The harvested energy can be stored in a supercapacitor and/or a rechargeable battery. Because energy can be harvested from the power cable continuously without any time constraint (such as day time only for PV panels), the storage capacity of the supercapacitor and/or battery can be much smaller than that for a solar power system. As the online monitoring system has to be mounted on the transmission tower (marked as ② in Fig. 1) that is earthed, there is a considerable transmission distance between the energy-harvesting point ① and the energy-receiving point ②. According to IEC 60137 Standard [20], the creepage distance depends on the voltage and the air pollution conditions as listed in Table I. Typical power requirements provided by a power company (Guangdong Power Grid Corporation, a subsidiary of China Southern Power Grid) are listed in Table II.

TABLE II
TYPICAL POWER REQUIREMENTS OF ONLINE MONITORING SYSTEMS
(COURTESY OF GUANGDONG POWER GRID CORPORATION)

	Sleep mode	Active mode
Video	2 W	12 W
Snow monitoring	1 W	3.5 W
Micrometeorological monitor	1 W	3 W
Microprocessing unit	10 mW	50 mW
Total:	4.01 W	18.55 W

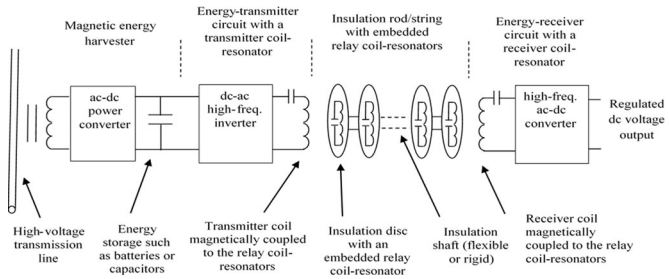

Fig. 2. Schematic of the novel WPT system for power systems [21].

Fig. 1 shows an example of rigid insulation strings holding the HV transmission lines to the transmission tower. For transmission distance of this magnitude, traditional 2-coil and 4-coil WPT techniques cannot achieve high efficiency because such efficiency is inversely proportional to the square of the transmission/insulation distance.

The new concept of WPT system for this HV application with large creepage distance is shown in Fig. 2. This concept consists of the following:

1) a magnetic field energy harvester with an energy storage element (such as supercapacitors and/or rechargeable batteries);
2) a dc–ac high-frequency power inverter driving a transmitter coil resonator;
3) a novel insulation rod/string with embedded relay coil resonators;
4) a high-frequency energy-receiving circuit with a receiver coil resonator.

In this study, the research focuses only on the new insulator string with embedded coil resonators for WPT. The front-stage energy harvesting module and the high-frequency ac-dc converter in the receiver stage will be covered in future research.

The novel insulation string consists of a series of insulation discs. If the discs are linked with rigid insulation shaft, a rigid insulation string (also known as "insulation rod") is formed. If the discs are linked with a flexible insulation shaft, the structure is called a flexible insulation string. The transmitter coil resonator is arranged in such a way that it is placed close to and magnetically coupled to the coil resonator in the first insulation disc on the transmitter side. Similarly, the last insulation disc of the insulation rod/string is placed close to the receiver's coil resonator for close magnetic coupling. The coil resonators embedded in the discs between the transmitter module and receiver module are used as relay or repeater coil resonators. The

Fig. 3. Schematic of a "*novel flexible insulation string*" consisting of novel discs (with a section of the toughed glass removed to show the embedded copper coil of the resonator).

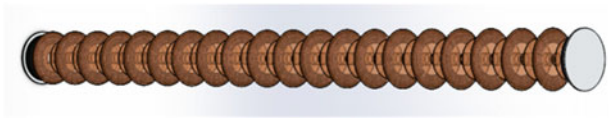

Fig. 4. Novel insulation string with (a) HVI and (b) WPT capabilities.

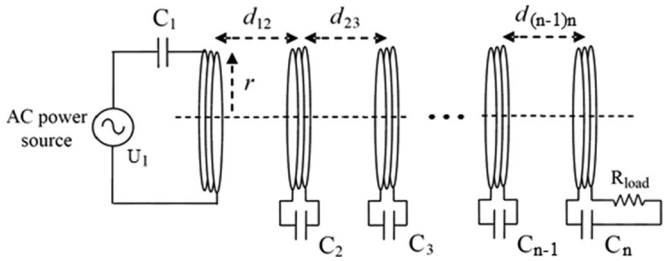

Fig. 5. *n*-coil domino system for wireless power transfer.

operation of the proposed insulation rod/string is based on the wireless domino-resonator systems [15], [16], which offer good compromise of high energy efficiency and transmission distance for midrange WPT applications.

III. ANALYSIS AND DESIGN OF AN INSULATION STRING WITH HVI AND WPT CAPABILITIES

A. Modeling of the Insulation String With Embedded Coil Resonators

Fig. 3 shows a typical structure of stackable discs in the form of an insulation string. Each disc has an embedded coil connected in series with a capacitor, forming an inductive-capacitive resonant tank (called coil resonators hereafter). The coil resonator is *totally enclosed* inside the insulation disc so that it is *not affected by dust and water*. The resonant frequency of this resonant tank in each disc should be identical. When many discs are connected in series as shown in Fig. 4, a new form of insulation string with HVI and WPT functions can be realized.

Consider a domino WPT system consisting of *n* coils as shown in Fig. 5. If we assume L_i is the self-inductance of the ith coil, R_i is the coil resistance of the ith coil, and M_{ij} is the mutual-inductance between the *i*th coil and the *j*th coil, then the system could be described by the matrix equation in (1) shown at the bottom of the next page.

If all the parameters in the system matrix in (1) as shown at the bottom of this page are known, for a given frequency *f*, we can get the input impedance of the system by giving a certain input of U_{1f}, calculating the input current I_{1f}, and then

$$Z_f = \frac{U_{1_f}}{I_{1_f}}. \tag{2}$$

Hence, a set of impedance values at different frequencies can be obtained: $Z_{f_1}, Z_{f_2}, \ldots, Z_{f_m}$, where f_i is one of the different frequencies, and Z_{f_i} is the input impedance at f_i

$$(Z_{f_1}, Z_{f_2}, \ldots, Z_{f_m}) = f \begin{pmatrix} L_1, L_2, \ldots, L_n, \\ M_{12}, M_{23}, \ldots, M_{(n-1)n}, \\ C_1, C_2, \ldots, C_n, \\ R_1, R_2, \ldots, R_n, \\ R_{\text{load}} \end{pmatrix} \tag{3}$$

Since the coils in the domino system are identical to each other, the self-inductance of L_1 through L_n can be treated as a constant value, and it could be accurately calculated [22]. The coil resistance, R_1 through R_n, can be considered as identical and it can be measured at the operating resonant frequency of the coil resonator. Such coil resistance can be considered as a constant value if the WPT system is operated around the resonant frequency. All the measured parameters or the nominal value of the resonators are shown in Table I. Meanwhile, we can treat the mutual inductances $M_{12}, M_{23}, \ldots, M_{(n-1)n}$ as functions of distances between each coil pair, $d_{12}, d_{23}, \ldots, d_{(n-1)n}$ [23], then (3) can be replaced bythe following equation:

$$(Z_{f_1}, Z_{f_2}, \ldots, Z_{f_{m-1}}, Z_{f_m}) = f \begin{pmatrix} L_1, L_2, \ldots, L_n, \\ d_{12}, d_{23}, \ldots, d_{(n-1)n}, \\ C_1, C_2, \ldots, C_n, \\ R_1, R_2, \ldots, R_n, \\ R_{\text{load}} \end{pmatrix}. \tag{4}$$

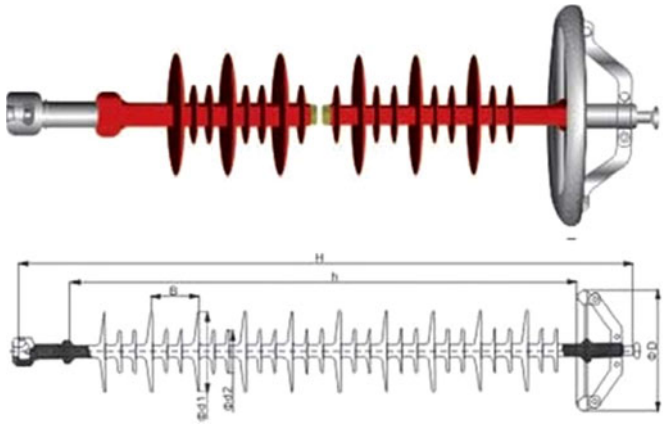

Fig. 6. Typical dimensions of a commercial insulation string [24].

The energy efficiency of the insulation string with embedded coil resonators is expressed as

$$\eta(f) = \frac{i_n^2(f) R_{load}}{i_n^2(f) R_{load} + \sum_{x=1}^{n} i_x^2(f) R_x} \tag{5}$$

and the output power is

$$P_{\text{out}}(f) = i_n^2(f) R_{\text{load}}. \tag{6}$$

B. Design of Coil Resonators Based on Practical Insulator Strings

The embeddable coil resonators of the proposed insulation string with WPT and HVI capability should preferably be compatible with the dimensions of existing insulation strings commercially available. Fig. 6 shows a practical example of a commercially available insulation string [24]. It consists of a series of insulation discs with large diameter separated by insulation discs with small diameter. The dimensions of the insulation string structure in this investigation are given in Table III, in which the distances between adjacent disc-*x* and disc-*y* with large diameters (labeled as "B" in Fig. 6) are tabulated as d_{xy}. The total distance of this example is 1.1 m and the diameter of the large disc is 0.2 m. The coil resonators are embedded only in the insulation discs of large diameters.

$$\begin{bmatrix} U_1 \\ 0 \\ \vdots \\ 0 \\ 0 \end{bmatrix} = \begin{bmatrix} R_1 + j\left(\omega L_1 - \frac{1}{\omega C_1}\right) & j\omega M_{12} & \cdots & j\omega M_{1(n-1)} & j\omega M_{1n} \\ j\omega M_{21} & R_2 + j\left(\omega L_2 - \frac{1}{\omega C_2}\right) & \cdots & j\omega M_{2(n-1)} & j\omega M_{2n} \\ \vdots & \vdots & \ddots & \vdots & \vdots \\ j\omega M_{(n-1)1} & j\omega M_{(n-1)2} & \cdots & R_{n-1} + j\left(\omega L_{n-1} - \frac{1}{\omega C_{n-1}}\right) & j\omega M_{(n-1)n} \\ j\omega M_{n1} & j\omega M_{n2} & \cdots & j\omega M_{n(n-1)} & R_n + R_l + j\left(\omega L_n - \frac{1}{\omega C_n}\right) \end{bmatrix} \begin{bmatrix} I_1 \\ I_2 \\ \vdots \\ I_{n-1} \\ I_n \end{bmatrix} \tag{1}$$

TABLE III
DESIGN PARAMETERS

d_{12} (m)	d_{23} (m)	d_{34} (m)	d_{45} (m)	d_{56} (m)	d_{67} (m)	d_{78} (m)	d_{89} (m)	d_{910} (m)	d_{1011} (m)	d_{1112} (m)
0.11	0.098	0.098	0.098	0.098	0.098	0.098	0.098	0.098	0.098	0.11

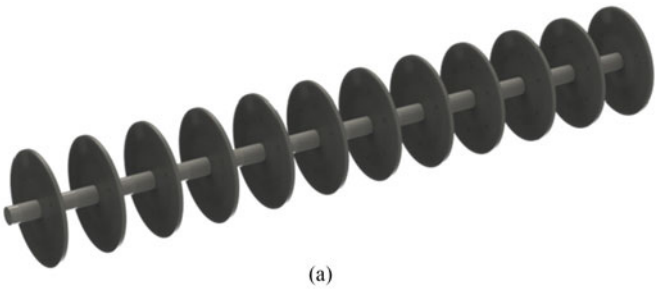

(a)

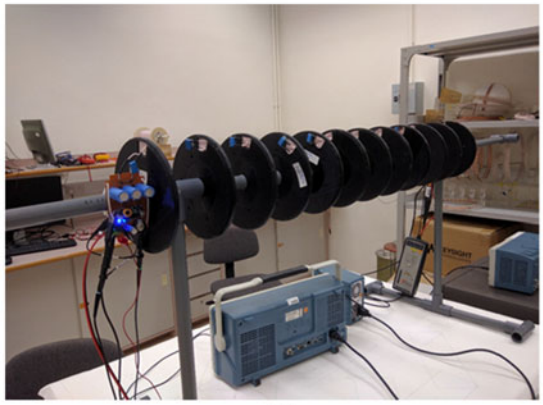

(b)

Fig. 7. Prototype of 12-coil insulator WPT system: (a) sketch and (b) real prototype.

IV. VERIFICATION AND EVALUATION OF THE WPT CAPABILITY

A. Practical Insulations String With Coil Resonators

Twelve coil resonators are designed to fit into the dimensions of the insulation discs of large diameter (i.e., 200 mm). The hardware setup is shown in Fig. 7. The energy efficiency of WPT system depends on the kQ product, where k is the coupling coefficient between adjacent magnetically coupled coils and Q is the quality factor of the coil. It is therefore necessary to use operating frequency high enough to achieve high Q factor within the capability of existing power electronics technology. The operating frequency is designed to be in the range from 300 to 500 kHz, which is within existing capability of switched mode power supplies.

The parameters of the coil resonator are tabulated in Table IV. Coils of such dimensions can be accommodated by existing insulation discs. The self-inductance is about 155 μH and the resonant capacitor is 1 nF. The targeted resonant frequency is about 400 kHz, at which the ac coil resistance is about 1.30 Ω and the Q factor is about 300. In order to improve the accuracy of the mathematical model, the actual capacitance values of the resonant capacitors and the separation distances between adjacent coil resonators are measured and tabulated in Table V. These measured values are used for computer-aided evaluation.

TABLE IV
PARAMETERS OF THE RESONATORS

Outer radius of windings	68 mm
Inner radius of windings	88 mm
Number of turns	24
Layer of the wire	2
Structure of the Litz wire	Φ 0.1 mm$*$120 strans Outer Φ 1.7mm
Inductance (calculated)	155.0 μH
Capacitance (nominal value) #1 through #12	1 nF
Measured wire resistance (at 400 kHz)	1.30 Ω

B. Computer-Aided Analysis With Practical Verification

1) Computed and Experimental Input Impedance and Input Phase Angle: In order to check the accuracy of the mathematical model described in the last section, the input impedance and the input phase angle of the insulation string prototype are measured with steps of 1 kHz increment from 300 to 500 kHz, when the last coil resonator is loaded with a fixed resistive load R_{laod} of 10 Ω. As multiple coil resonator system is a high-order system with multiple resonant points, 200 sets measurements from 300 to 500 kHz are captured with a high-speed digital oscilloscope and transferred to a computer for analysis. Fig. 8 shows the simulated and experimental results of the impedance (Z_exp and Z_sim) over the specific frequency range. The corresponding simulated and measured phase angle between input voltage and current are shown in Fig. 9. These results indicate that the overall impedance has a transitional change from being capacitive-resistive (below 380 kHz) to resistive (at around 380– 400 kHz) and then inductive-resistive (above 400 kHz) as the frequency increases from 300 to 500 kHz. These measurements show that the resonant frequency of the overall system is within 380–400 kHz, which is close to the targeted frequency of 400 kHz. The good agreements between the experimental and simulated results confirm the validity of the mathematical model. This provides the confidence that the mathematical model can be used to optimize the system operating conditions.

2) Computed and Experimental Energy Efficiency: Computer analysis can be used to explore the relationships among the energy efficiency, operating frequency, and load resistance for optimal operation in a three-dimensional (3-D) manner. In the practical setup, a high-frequency power source is used to drive the transmitter coil, while the last resonator is loaded with a resistor. Because no power converter is involved in the process, the energy efficiency is calculated from the ratio of the load power and the input power to the transmitter coil. Under an excitation voltage of 28 V, such 3-D plot is shown in Fig. 10(a). This result shows that energy efficiency exceeding 60% is possible for transmitting more than 25 W over an overall transmission distance of 1.1 m based on the proposal insulation string structure with large insulation discs embedded with coil resonators. In

TABLE V
PRACTICAL PARAMETERS OF THE RESONANT CAPACITANCE AND SEPARATION DISTANCES

C_1 (μF)	C_2 (μF)	C_3 (μF)	C_4 (μF)	C_5 (μF)	C_6 (μF)	C_7 (μF)	C_8 (μF)	C_9 (μF)	C_{10} (μF)	C_{11} (μF)	C_{12} (μF)
1.05	1.01	1.03	1.02	1.02	1.03	1.01	1.03	1.04	0.99	0.98	1.06

d_{12} (m)	d_{23} (m)	d_{34} (m)	d_{45} (m)	d_{56} (m)	d_{67} (m)	d_{78} (m)	d_{89} (m)	d_{910} (m)	d_{1011} (m)	d_{1112} (m)
0.113	0.099	0.095	0.098	0.100	0.096	0.096	0.098	0.095	0.085	0.117

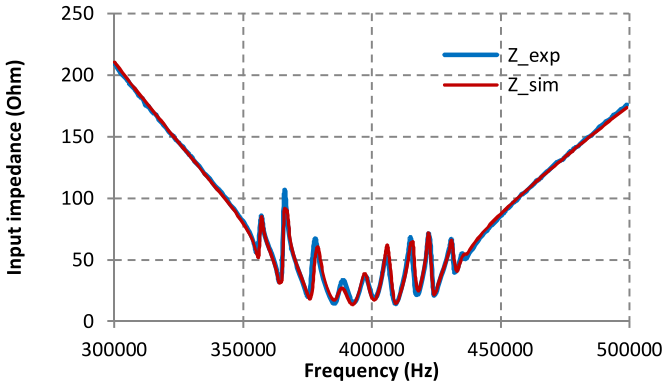

Fig. 8. Experimental and simulated values of the input impedance.

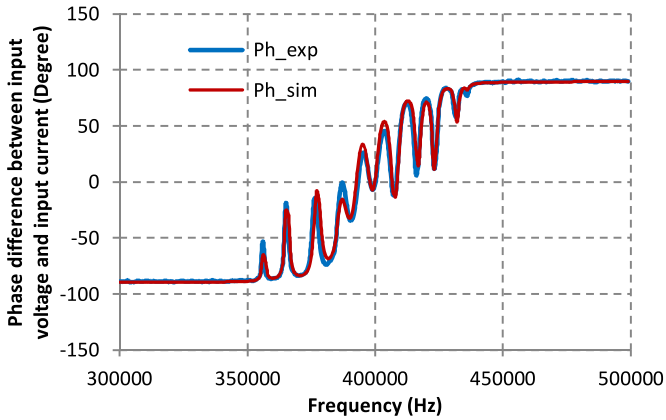

Fig. 9. Experimental and simulated values of the phase angle of the input impedance.

order to examine the details of this result, the energy efficiency of the prototype is included in a 2-D contour plot as shown in Fig. 10(b). This computed result indicates that high energy efficiency can be achieved for this prototype over a wide load resistance range with the frequency range of 380–400 kHz. For example, if an operating frequency of 393 kHz is selected, high energy efficiency can be achieved for a load resistance range from about 8 to 50 Ω.

For a load resistance of 50 Ω, the computed and measured energy efficiency curves over a frequency range from 340 to 440 kHz are plotted in Fig. 11. The good agreement between the computed and practical measurement confirm that the accuracy of the mathematical model is acceptable and the energy efficiency exceeding 60% is practically feasible for a transmission distance of 1.1 m.

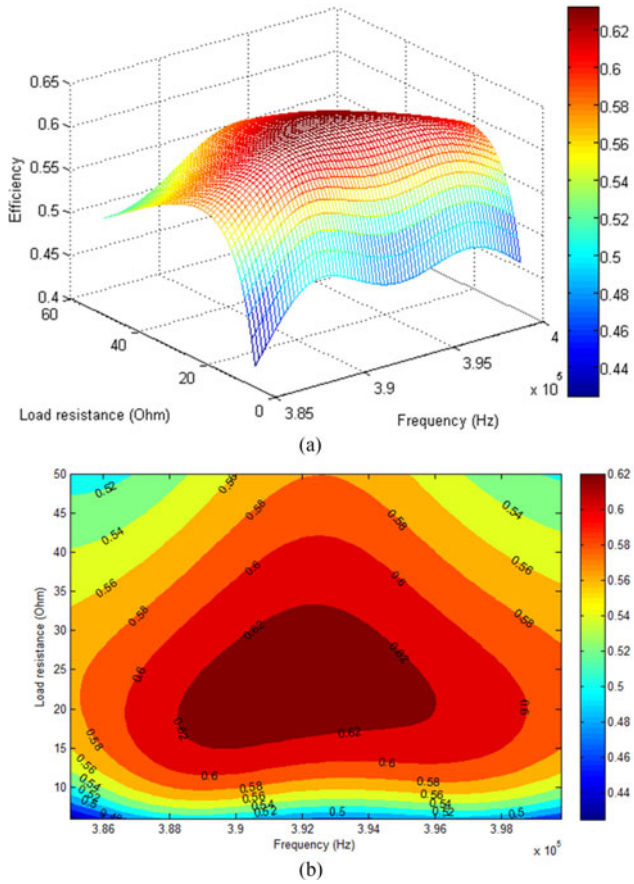

Fig. 10. Computed energy efficiency of the prototype as a function of operating frequency and load resistance (input voltage: 28 V): (a) 3-D plot and (b) 2-D contour plot.

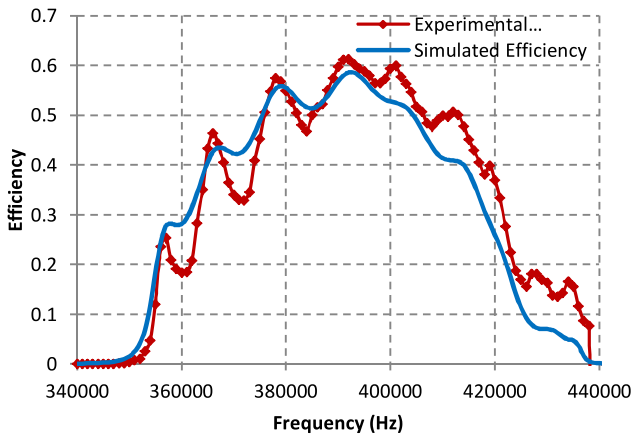

Fig. 11. Computed and experimental energy efficiency of the prototype load with a resistor of 50 Ω.

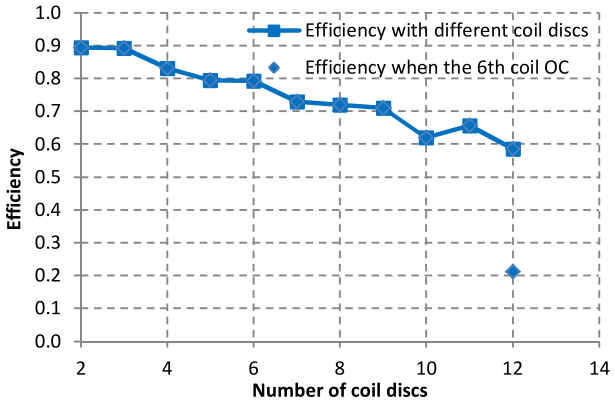

Fig. 12. Energy efficiency with different coil discs at operating frequency of 393 kHz with a load resistance of 50 Ω (with one extra measured point of energy efficiency when the 6th coil of a 12-coil WPT system open circuited).

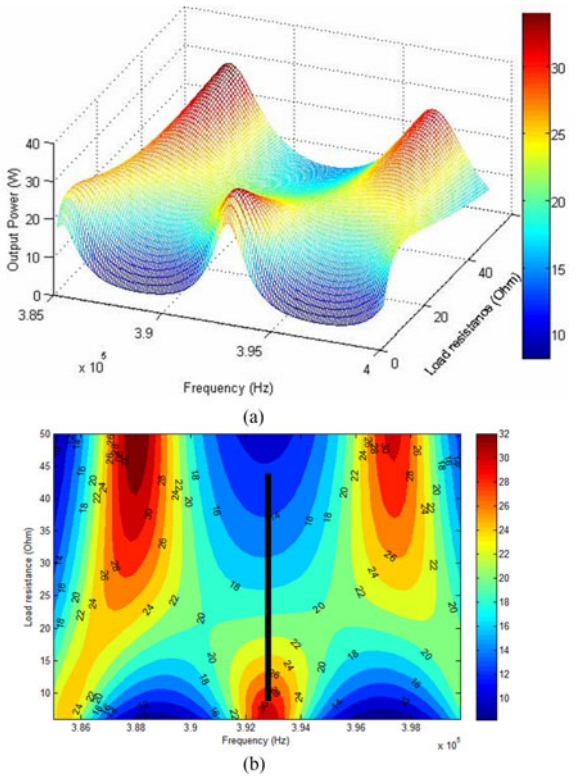

Fig. 13. Computed output power as a function of the operating frequency and load resistance (input voltage: 28 V): (a) Computed output power in a 3-D plot; (b) Computed output power in a 2-D contour plot. [Note: The bold line illustrates the load resistance range under consideration in Figs.14 and 15].

The variation of the energy efficiency as a function of the distance (or number of insulation discs) has been evaluated. The load is placed at each insulated disc from the second to the last coil resonator in a 12-coil WPT system (with a total distance of 1.1 m between the transmitter coil resonator to the last receiver coil resonator). The energy efficiency curve is plotted in Fig. 15. It can be seen that the energy efficiency varies from about 90% to about 60% in this practical prototype. One extra test has also been conducted in a 12-coil system with the sixth coil open-circuited (i.e., the transmission distance between the fifth and seventh coil resonator is now doubled). This special energy

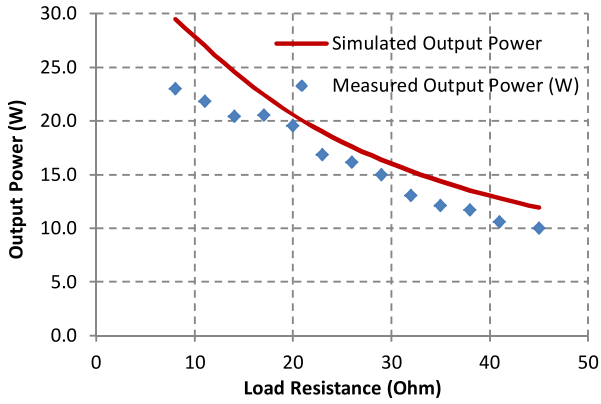

Fig. 14. Experimental output power over a range of load resistance at an operating frequency of 393 kHz and an input voltage of 28.3 V. [Note: Parasitic inductance in the load resistor at 393 kHz is not considered in the simulation].

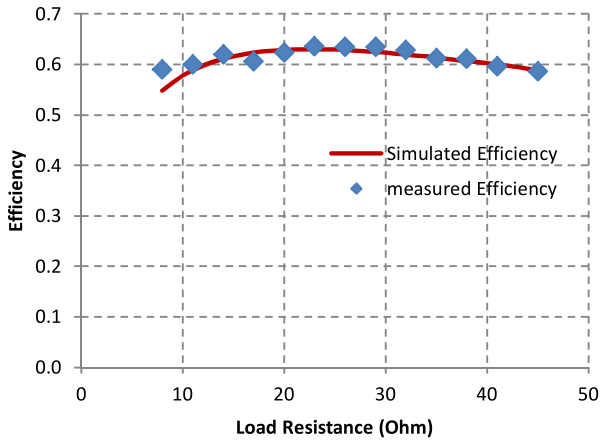

Fig. 15. Experimental energy efficiency over a range of load resistance at an operating frequency of 393 kHz and an input voltage of 28.3 V.

efficiency is included in Fig. 12. It is noted that wireless power can still be transmitted to the load, but the energy efficiency will drop from about 60% to about 20%.

3) Computed and Measured Output Power: The output power as a function of the operating frequency and load resistance has also been computed as shown in a 3-D plot in Fig. 13(a). The phenomenon of frequency splitting can be observed. In order to make it easy to design the operating range, the output power is displayed in a 2-D plane against the color scale in Fig. 13(b), in which the load resistance range from 8 to 45 Ω is highlighted in a solid line at 393 kHz.

Practical tests have been conducted with the prototype operating along the load resistance range from 8 to 45 Ω at 393 kHz. The experimental and simulated output power is plotted in Fig. 14. It is noted that the practical output power is slightly less than the predicted one. At high-frequency operation, some inductive effect exists in the ceramic resistor. Such parasitic inductance increases the effective impedance of the output load and reduces the output power. However, the overall trend of the actual power is consistent with the predicted curve. The corresponding energy efficiency results over this load range are shown in Fig. 15. These results confirm that an energy efficiency exceeding 60% is possible over a wide load range.

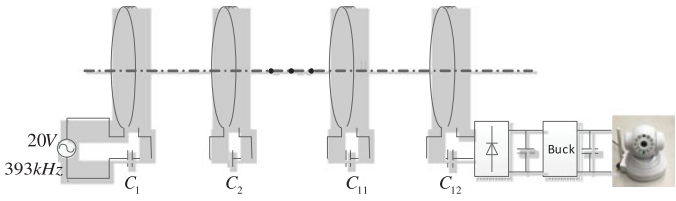

Fig. 16. Diagram of the insulator WPT system.

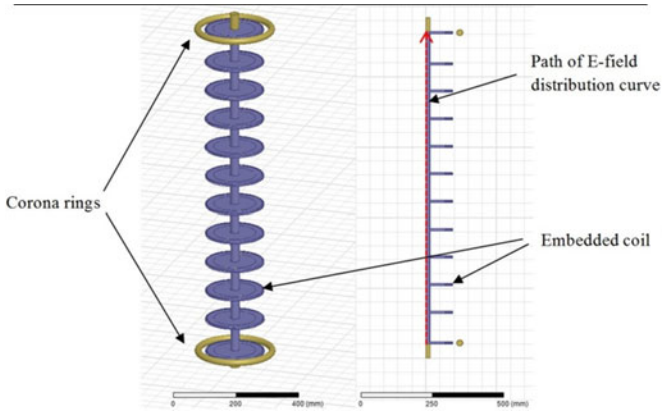

Fig. 17. 3-D structure (left) and 2-D finite-element model (right) of the insulator string.

TABLE VI
PARAMETERS OF THE 110 KV COMPOSITE INSULATOR

Diameter of the large sheds	190 mm
Spacing of the large sheds (average)	100 mm
No. of the large sheds	12
Minimum arcing distance	1100 mm
Minimum nominal creepage distance	2710 mm

C. Practical Demonstration of Powering Online Monitoring Camera

The WPT prototype has been used to drive an IP camera (Brand: WIRYTH) as shown in Fig. 16. An ac power source of 20 V at 393 kHz is used to drive the insulation string WPT system. A simple ac/dc converter and a buck converter are used to maintain the output voltage of 5 V dc to fit the requirement of the IP camera. The normal operating current of the IP camera is 300 mA and the maximum current is 1300 mA @ 5 V input when the camera is rotating. A video of the live demonstration is included in the attached video file.

V. SIMULATION STUDY OF ELECTRIC FIELD DISTRIBUTION

While the main theme of this study focuses on the WPT capabilities of this proposed idea, a finite-element simulation study has been conducted to evaluate the electric field distribution of the proposed insulation string with and without the embedded coil resonators. Finite element analysis is carried out on a 110-kV insulator prototype. The dimension of the prototype is based on that of a commercially available 110-kV composite insulator which has 12 pieces of large sheds. The parameters of a practical 110-kV composite insulator (see Fig. 17) listed in Table VI are used in the finite-element simulation.

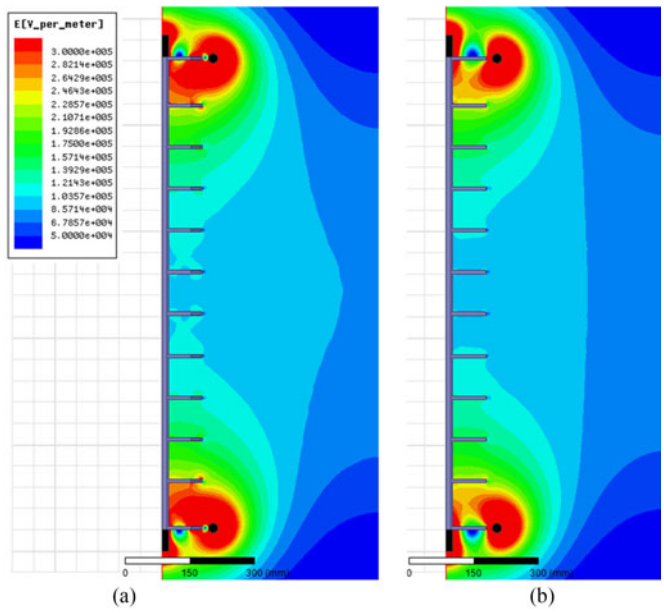

Fig. 18. Simulated electric field distributions of the insulation strings: (a) *with* and (b) *without* embedded coil resonators.

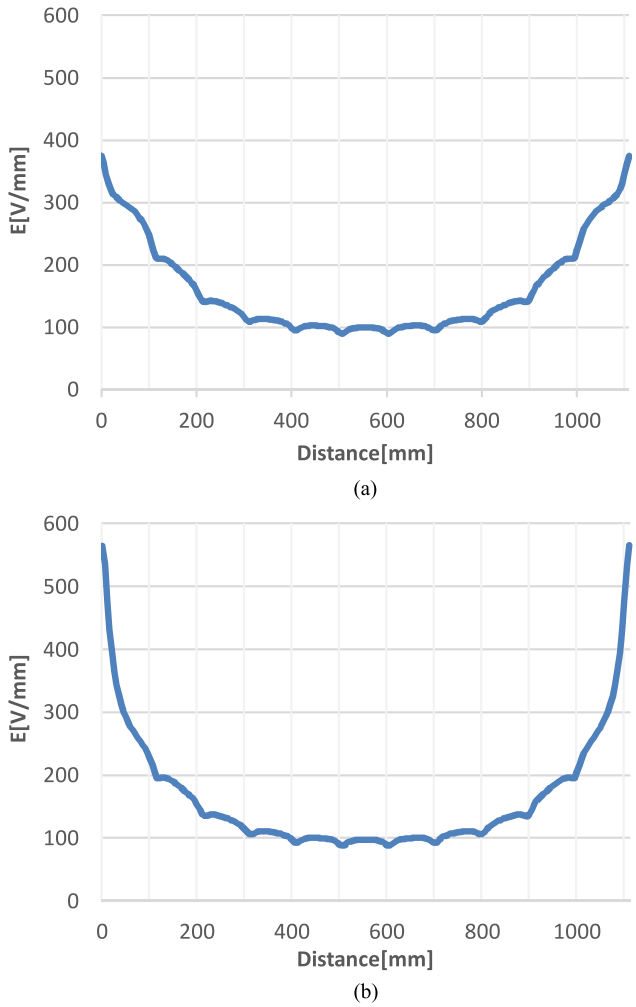

Fig. 19. Simulated axial E-field distribution along the surface of the rod: (a) *with* and (b) *without* embedded coil resonators.

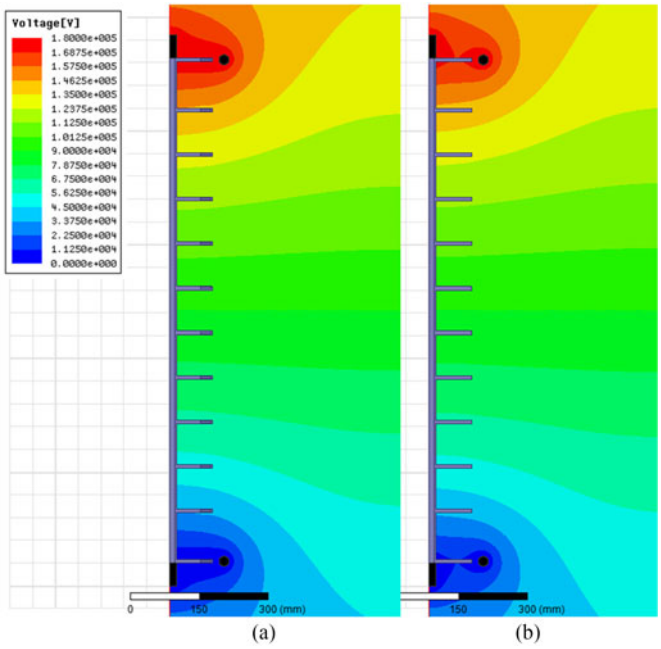

Fig. 20. Simulated voltage distribution of the insulators: (a) *with* and (b) *without* the embedded coil resonators.

Fig. 17 shows the 3-D structure and 2-D simulation model of the prototype. When adding coils for WPT, two more sheds are added for holding the transmitter coil and the receiver coil. In the analysis, the insulator string with embedded coils and two more sheds are compared with the original insulator. Applying the same 180-kV peak voltage to these two insulators, the E-field distribution situations are compared in Figs. 18–20. Fig. 18 shows that the E-field distribution over the whole area is more even for the insulator string with embedded coils. The curves in Fig. 19(a) and (b) also indicate that the E-field intensity at two ends of the insulator string is lower for the case with the embedded coil resonators. Fig. 20 shows that the voltage distribution has a similar pattern for with and without the embedded coil resonators. Therefore, it can be inferred that adding coils to the insulator does not seem to degrade the whole E-field or voltage distribution. Instead, the coils near the corona rings might have a function of further evening the E-field distribution at two ends. Practical high-voltage tests will be conducted in the future to confirm these simulation results.

VI. Conclusion

This paper presents a novel concept of using a HVI string structure with embedded coil resonators for wireless power application. This idea is proposed for an industrial application of WPT for powering online monitoring system in high-voltage transmission networks. The WPT aspects of this idea have been studied with the help of a computer-aided analysis and practically verified. It has been found that more than 25 W can be practically transferred over an overall transmission distance of 1.1 m at an energy efficiency exceeding 60%. This amount of power is sufficient to meet the typical power requirement of 25 W in many existing online monitoring systems. This paper contains the first set of experimental results for this online monitoring application. A finite-element simulation on the electric field distribution has been conducted. The simulated results suggest no special problem in its HVI capability. Further research is being conducted to evaluate the WPT capability in a high-voltage environment.

Acknowledgment

The practical power requirements of online monitoring systems are provided by Guangdong Power Grid Corporation. The patent application [21] was supported by the University of Hong Kong.

References

[1] China.org.cn, "Blackouts hit 17 provinces," China.org.cn, Beijing, China, [Online]. Available: http://www.china.org.cn/english/China/241448.htm, Accessed on: Jan. 31, 2008.

[2] Typhoon Mujigae kills 11 in south china, cuts off power," [Online]. Available: http://www.chinadaily.com.cn/china/2015-10/06/content_22109076.htm, Accessed on: Oct. 6, 2015.

[3] X. Sun, Q. Huang, L. J. Jiang, and P.W. T. Pong, "Overhead high-voltage transmission-line current monitoring by magnetoresistive sensors and current source reconstruction at transmission tower," *IEEE Trans. Magn.*, vol. 50, no. 1, Jan. 2014, Art. no. 4000405.

[4] Kai Han and H. Xu, "Research on wireless network-based power line inspection," in *Proc. 2009 Int. Forum Inf. Tech. Appl.*, 2009, pp. 379–381.

[5] X. Wang, J. Hu, B. Wu, L. Du, and C. Sun, "Study on edge extraction methods for image-based icing on-line monitoring on overhead transmission lines," in *Proc. 2008 Int. Conf. High Voltage Eng. Appl.*, Chongqing, China, Nov. 9–13, 2008, pp. 661–665.

[6] T. Yin, X. Chen, Du Yan, and Y. He, "Research on power supply employed in ices real-time monitoring system of high-voltage transmission lines," in *Proc. 2008 Int. Conf. High Voltage Eng. Appl.*, Chongqing, China, Nov. 9–13, 2008, pp. 626–628.

[7] X. Huang and X. Wei, "New on-line monitoring technology of transmission line conductor icing," in *Proc. 2012 IEEE Int. Conf. Condition Monit. Diag.*, Bali, Indonesia, Sep. 23–27 2012, pp. 581–585.

[8] J. Yang Z. Dai, and Q. Yu, "Online monitoring of wind-induced vibration of transmission steel high tower," in *Proc. 2011 Asia-Pac. Power Energy Eng. Conf.*, Mar. 25–28 2011, pp. 1–4.

[9] R. Holmukhe, P. Chaudhari, P. Kulkarni, K. Deshpande, and P. Kulkarni, "Measurement of weather parameters via transmission line monitoring system for load forecasting," in *Proc. 3rd Int. Conf. Emerg. Trends Eng. Tech.*, 2010, p. 298–303.

[10] S. Yang, H. Li, W. Zhou, and J. Yu, "Lightning current waveform observed on transmission line and lightning tower in china," in *Proc. Int. Conf. Lightning Protection*, Shanghai, China, 2014, pp. 35–39.

[11] X. Huang, W. Li, and Y. Zhang, "Research of transmission line tower anti-theft monitoring technique based on video difference analysis," in *Proc. 8th Int. Conf. Wireless Commun., Netw. Mobile Comput.*, 2012, pp. 1–4.

[12] R. Berthiaume and R. Blais, "Microwave repeater power supply tapped from the overhead ground wire on 735 kV transmission lines," *IEEE Trans. Power App. Syst.*, vol. PAS-99, no. 1, pp. 183–184, Jan./Feb. 1980.

[13] A. Kurs, A. Karalis, R. Moffatt, J. D. Joannopoulos, P. Fisher, and M. Soljacic, "Wireless power transfer via strongly coupled magnetic resonances," *Science*, vol. 317, no. 5834, pp. 83–86, Jul. 2007.

[14] S. Y. R. Hui, W. X. Zhong, and C. K. Lee, "A critical review of recent progress in mid-range wireless power transfer," *IEEE Trans. Power Electron.*, vol. 29, no. 9, pp. 4500–4511, Sep. 2014.

[15] S. Y. R. Hui and W. X. Zhong, "Apparatus and method for wireless power transfer," Patent PCT/IB2011/000050, Jan. 14, 2011.

[16] W. X. Zhong, C. K. Lee, and S. Y. R. Hui, "General analysis on the use of Tesla's resonators in domino forms for wireless power transfer," *IEEE Trans. Ind. Electron.*, vol. 60, no. 1, pp. 261–270, Jan. 2013.

[17] C. K. Lee, W. X. Zhong, and S. Y. R. Hui, "Effects of magnetic coupling of non-adjacent resonators on wireless power domino-resonator systems," *IEEE Trans. Power Electron.*, vol. 27, no. 4, pp. 1905–1916, Apr. 2012.

[18] W. X. Zhong, C. K. Lee, and S. Y. R. Hui, "Wireless power domino-resonator systems with non-coaxial axes and circular structures," *IEEE Trans. Power Electron.*, vol. 27, no. 11, pp. 4750–4762, Nov. 2012.

[19] C. Zhang, N. Tang, W. X. Zhong, C. K. Lee, and S. Y. R. Hui, "A new energy harvesting and wireless power transfer system for smart grid," in *Proc. IEEE 7th Int. Symp. Power Electron. Distrib. Gen. Syst.*, Vancouver, BC, Canada, Jun. 27–30, 2016, pp. 2329–5767.
[20] *Insulated Bushings for Alternating Voltages Above 1000V*, IEC 60137 International Standard, 2003.
[21] S. Y. R. Hui and C. Zhang, "A wireless power transfer system," U.S. Provisional Patent 62/256,726, Nov. 18, 2015.
[22] S. Babic, F. Sirois, C. Akyel, and C. Girardi, "Mutual inductance calculation between circular filaments arbitrarily positioned in space: Alternative to Grover's formula," *IEEE Trans. Magn.*, vol. 46, no. 9, pp. 3591–3600, Sep. 2010.
[23] C. Zhang, W. X. Zhong, X. Liu, and S. Y. R. Hui, "A fast method for generating time-varying magnetic flux patterns of mid-range wireless power transfer systems," *IEEE Trans. Power Electron.*, vol. 30, no. 3, pp. 1513–1520, Mar. 2015.
[24] Wish Composite Insulator Corporation, Ltd., Xi'an, China, [Online]. Available: http://wishpower.net/enproduct/show.asp?id=178
[25] S. Y. R. Hui, "Magnetic resonance for wireless power transfer [a look back]," *IEEE Power Electron. Mag.*, vol. 3, no. 1, pp. 14–31, Mar. 2016.
[26] C. Park, S. Lee, G.-H. Cho, and C. T. Rim, "Innovative 5-m-off-distance inductive power transfer systems with optimally shaped dipole coils," *IEEE Trans Power Electron.*, vol. 30, no. 2, pp. 817–827, Feb. 2015.

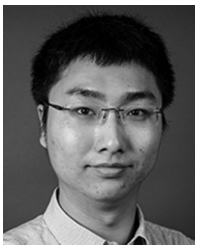

Cheng Zhang (S'13–M'16) was born in China, in 1990. He received the B.Eng. degree (first class Hons.) in electronic and communication engineering from the City University of Hong Kong, Hong Kong, in 2012 and the Ph.D. degree in electronic and electrical engineering from The University of Hong Kong, Hong Kong, in 2016.

From 2016 to 2017, he was a Senior Research Assistant in the Department of Electrical and Electronic Engineering, The University of Hong Kong. He is currently a Postdoctoral Research Associate in the Research Laboratory of Electronics, Massachusetts Institute of Technology, Cambridge, MA, USA. His research interests include high-frequency ac–dc power conversions and designs and optimizations for wireless power transfer applications.

Deyan Lin (M'09) received the B.Sc. and M.A.Sc. degrees in electrical engineering from Huazhong University of Science and Technology, Wuhan, China, in 1995 and 2004, respectively, and the Ph.D. degree from the City University of Hong Kong, Hong Kong, in 2012.

He is currently a Professor in the School of Automation, Wuhan University of Technology, Wuhan, China and a Postdoctoral Fellow in the Department of Electrical and Electronic Engineering, The University of Hong Kong, Hong Kong. From 1995 to 1999, he was a Teaching Assistant in the Electrical Engineering Department, Jianghan University, Wuhan, China, where he became a Lecturer in 1999. From 2008 to 2009, he was a Senior Research Assistant at the City University of Hong Kong. His research interests include wireless power transfer, memristors, modeling, and control of gas-discharge lamps and light-emitting diode technology.

Niang Tang was born in Hunan, China in 1984. He received the B.S. and M.S. degrees from Changsha University of Science and Technology, Changsha, China and the Ph.D. degree from North China Electric Power University, Beijing, China, in 2006, 2009, and 2013, respectively, all in electrical engineering.

He is currently working in the Electric Power Research Institute of Guangdong Power Grid Corporation, Ltd., Guangzhou, China. His research interests include power electronics and power quality.

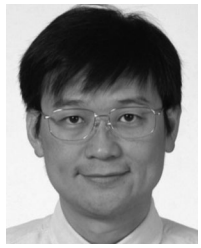

S. Y. Ron Hui (M'87–SM'94–F'03) received the B.Sc. (Eng.) Hons. degree in electrical and electronic engineering from the University of Birmingham, Birmingham, U.K., in 1984, and the D.I.C. and Ph.D. degrees in electrical and electronic engineering from Imperial College London, London, U.K., in 1987.

He currently holds the Philip Wong Wilson Wong Chair Professorship at the University of Hong Kong, Hong Kong, and a part-time Chair Professorship at Imperial College London, London, U.K. He has published more than 300 technical papers, including more than 230 refereed journal publications. More than 60 of his patents have been adopted by the industry. His inventions on wireless charging platform technology underpin key dimensions of Qi, the world's first wireless power standard, with freedom of positioning and localized charging features for wireless charging of consumer electronics.

Dr. Hui is an Associate Editor of the IEEE TRANSACTIONS ON POWER ELECTRONICS and the IEEE TRANSACTIONS ON INDUSTRIAL ELECTRONICS, and the Editor of the IEEE JOURNAL OF EMERGING AND SELECTED TOPICS IN POWER ELECTRONICS. He, in November 2010, received the IEEE Rudolf Chope R&D Award from the IEEE Industrial Electronics Society and the IET Achievement Medal (The Crompton Medal). He also received the 2015 IEEE William E. Newell Power Electronics Award. He is a Fellow of the Australian Academy of Technology & Engineering and a Fellow of the Royal Academy of Engineering, London, U.K.